Variational Quantum Simulators Based on Waveguide QED

C. Tabares, A. Muñoz de las Heras, L. Tagliacozzo, D. Porras, and A. González-Tudela*
Institute of Fundamental Physics IFF-CSIC, Calle Serrano 113b, 28006 Madrid, Spain

(Received 9 February 2023; revised 28 April 2023; accepted 3 July 2023; published 14 August 2023)

Waveguide QED simulators are analog quantum simulators made by quantum emitters interacting with one-dimensional photonic band gap materials. One of their remarkable features is that they can be used to engineer tunable-range emitter interactions. Here, we demonstrate how these interactions can be a resource to develop more efficient variational quantum algorithms for certain problems. In particular, we illustrate their power in creating wave function *Ansätze* that capture accurately the ground state of quantum critical spin models (XXZ and Ising) with fewer gates and optimization parameters than other variational *Ansätze* based on nearest-neighbor or infinite-range entangling gates. Finally, we study the potential advantages of these waveguide *Ansätze* in the presence of noise. Overall, these results evidence the potential of using the interaction range as a variational parameter and place waveguide QED simulators as a promising platform for variational quantum algorithms.

DOI: 10.1103/PhysRevLett.131.073602

Introduction.—Variational quantum algorithms (VQAs) [1,2] aim at exploiting current noisy intermediate scale quantum (NISQ) devices [3] before the fault-tolerant era arrives. Such algorithms leverage the power of classical optimizers to find the combination of single-qubit and multiqubit gates (i.e., constructing a parametrized quantum circuit, or *Ansatz*) that miminizes a given cost function. The cost function is generally the expectation value of an operator in a state constructed using the parametrized quantum circuit and measured in the quantum hardware. One paradigmatic example is the variational quantum eigensolver (VQE) [4] in which the cost function is the energy of a given many-body Hamiltonian, e.g., in quantum chemistry [5–11] or high-energy physics problems [12–16], among others. However, by changing the cost function, VQAs can also solve combinatorial optimization problems [17–22] and be applied to quantum machine learning [23,24] or quantum metrology protocols [25–28].

Like in classical variational approaches, the power of a VQA depends crucially on the *Ansatz*. First, the *Ansatz* needs to be expressive enough to accurately capture the solution of the problem targeted. While adding more gates allows us to cover a wider Hilbert space region, circuits featuring a small number of them offer both a reduced complexity when estimating cost functions and their gradients through measurements [4], and are less prone to errors. Thus, an *Ansatz* should ideally reproduce the phenomena of interest with as few gates as possible. Additionally, it should avoid the barren-plateau problem, i.e., the flattening of the optimization landscape, especially critical as the number of qubits increases [29] and for highly expressive *Ansätze* [30]. State-of-the-art *Ansätze* divide between hardware-efficient *Ansätze* (HEA) [6], motivated by the connectivities of the devices, and problem-tailored *Ansätze*, such as unitary-coupled cluster [5] or Hamiltonian variational *Ansätze* (HVAs) [31–35], which are inspired by the problem structure. While the former are more naturally implemented in state-of-the-art NISQ devices, the latter are easier to optimize because their structure allows us to avoid barren plateaus while being expressive enough to capture the solution [35]. However, such problem-inspired VQAs are also limited by the current hardware connectivities. Thus, despite many proof-of-principle VQA illustrations [5,6,12,36], none of the *Ansätze* considered fully solved all existing challenges. This is why the search for more efficient *Ansätze* is one of the most pressing questions in the NISQ era.

In this Letter, we introduce and characterize a different type of *Ansatz* inspired by the interactions that can be obtained in structured waveguide QED (wQED) setups [37–54]. These are systems where quantum emitters interact with one-dimensional photonic modes with nonlinear energy dispersions [see Fig. 1(a)]. When the emitters' optical transition frequency lies within a photonic band gap, the waveguide modes induce coherent, tunable-range interactions [55–57] which can be used to engineer multiqubit entangling gates between the emitters. Here, we build *Ansätze* combining such tunable-range gates with single-qubit rotations [see Fig. 1(b)] and implement the VQE to show that they can represent the ground states (g.s.) of critical spin models with fewer gates than existing *Ansätze*. The key difference between the wQED *Ansatz* and existing ones is the possibility to dynamically tune the interaction range, which we take as a variational parameter. This allows the algorithm to find states displaying long-range correlations with fewer gates than the standard fixed-range connectivities *Ansätze*. Finally, we study the impact of the reduced number of gates in the presence of noise.

 © 2023 American Physical Society

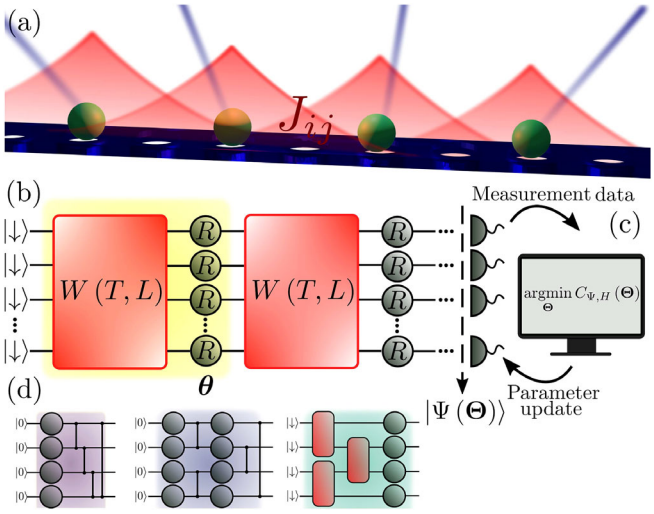

FIG. 1. (a) Atoms (green) with optical transitions in waveguide band gap regions form photonic bound states (red), leading to tunable-range emitter interactions $J_{ij} \sim e^{-|x_i-x_j|/L}$ that can be controlled using external lasers (blue). (b) Taking the atoms as qubits, these interactions generate an entangling operation (red) which can be combined with single-qubit rotations $R(\boldsymbol{\theta})$ to build a layer (yellow) of a variational quantum circuit that generates the state $|\Psi(\boldsymbol{\Theta})\rangle$. (c) The measurement of an observable H over this state defines a cost function $C_{\Psi,H}(\boldsymbol{\Theta})$ that is minimized using a classical processor. (d) Scheme of other relevant circuits with first-neighbor entangling gates, such as the hardware-efficient *Ansatz* (HEA) (purple), the brick-layer *Ansatz* (dark blue), and the Hamiltonian variational *Ansatz* (HVA) (light blue).

wQED Ansatz.—The physical setup we consider is summarized in Fig. 1(a). It consists of several emitters that can be individually or globally addressed by lasers, coupled to a one-dimensional waveguide. Although we depict the emitters as atoms and the waveguide as a photonic-crystal one [58,59], our findings can be extrapolated to other wQED platforms with different emitters (e.g., solid-state emitters [41–47]) and/or waveguides (such as microwave materials [48–52] or matter-wave waveguides [53,54]). Assuming the emitters couple to the waveguide modes through an effective transition between two states g and e whose frequency lies in the band gap, and under the conditions in which the photonic field can be adiabatically eliminated, the dynamics of the emitters are described by the following Hamiltonian [55–57]:

$$H_{XX} = J_{XX} \sum_{i \neq j} e^{-|x_i - x_j|/L} \sigma^i_{eg} \sigma^j_{ge}, \tag{1}$$

where J_{XX} is the interaction strength, L its effective range, which depends on the detuning between the effective transition frequency and the band edge and thus can be dynamically tuned [60–62], x_i is the atomic position, and $\sigma^i_{ge} = |g\rangle_i\langle e|_i$ the transition dipole operator. Similarly, as shown in Refs. [55–57] and Supplemental Material (SM) [63], if the emitters have two optically excited states that couple to the waveguide modes, one can also obtain an effective Hamiltonian $H_I = J_I \sum_{i \neq j} e^{-|x_i - x_j|/L} \sigma^i_x \sigma^j_x$, with $\sigma^i_x = (\sigma^i_{eg} + \sigma^i_{ge})/2$ the Pauli matrix in the x direction. Applying these Hamiltonians for a time t, one can obtain multiqubit gates described by the unitaries $W_{XX}(T,L) = e^{-itH_{XX}}$ or $W_I(T,L) = e^{-itH_I}$, respectively. Such gates can be parametrized by two tunable parameters [see Fig. 1(b)]: the normalized interaction time $T = tJ$ (with J being either J_{XX} or J_I) and its range L. To build our wQED *Ansätze*, we concatenate these unitaries with single-qubit rotations, e.g., in the z direction, described by the unitary $R(\boldsymbol{\theta}) = \prod_{j=1}^{N} e^{-i\theta_j \sigma^j_z}$, where $\boldsymbol{\theta} = (\theta_1, \theta_2, \ldots)$. The wQED *Ansatz* consists of D repetitions or *layers* of this combination of single- and multiqubit unitaries, see Fig. 1(b), described by the global unitary:

$$U_{\text{wQED}-\alpha}(\boldsymbol{\Theta}) = \prod_{i=1}^{D} R_i(\boldsymbol{\theta}^i) W_{i,\alpha}(T_i, L_i), \tag{2}$$

where $\boldsymbol{\Theta} = (\boldsymbol{\theta}, \boldsymbol{T}, \boldsymbol{L})$ is a vector embedding all variational parameters, and $\alpha = XX$ or I depending on the coupling configuration chosen. All these parameters can be modified independently: for instance, in simple two-level systems L can be tuned through the detuning and T adjusted accordingly using the physical time of the interaction t, or the strength of the photon-mediated interaction J (see Ref. [63]).

VQE with wQED Ansätze.—The main steps of VQE are as follow [4] (further explanations can be found in the SM [63]). (i) The multiqubit system is initialized in a state $|\Psi_0\rangle$. (ii) The initial state is the input of a parametrized quantum-circuit *Ansatz* described by a unitary $U(\boldsymbol{\Theta})$, for some initial choice of variational parameters $\boldsymbol{\Theta}$. The output is a final state $|\Psi(\boldsymbol{\Theta})\rangle = U(\boldsymbol{\Theta})|\Psi_0\rangle$. (iii) The cost function, i.e., the expectation value of the many-body Hamiltonian $C(\boldsymbol{\Theta}) = \langle\Psi(\boldsymbol{\Theta})|H|\Psi(\boldsymbol{\Theta})\rangle$, is obtained. (iv) Finally, the value of $C(\boldsymbol{\Theta})$ is fed to a classical optimizer that updates the parameters. This procedure is repeated until the energy does not change significantly, meaning that VQE has found the optimal parameters $\boldsymbol{\Theta}_{\text{opt}}$ that minimize the energy of H, unless it gets stuck in some local minima [29,30]. Thus, this value of the energy is an upper bound to the actual value of the g.s. energy.

In what follows, we apply this procedure to several quantum-critical spin models. These constitute interesting benchmarks as their g.s. feature long-range correlations, which are the most challenging to capture for classical and quantum algorithms [80–82]. We use an adiabatically assisted VQE algorithm [83], explained in detail in SM [63], and compare the performance of the wQED *Ansätze* against the most popular fixed-structure *Ansätze* of the literature [see Fig. 1(d) for a schematic picture of their circuits]: a hardware-efficient *Ansatz* [6] based on

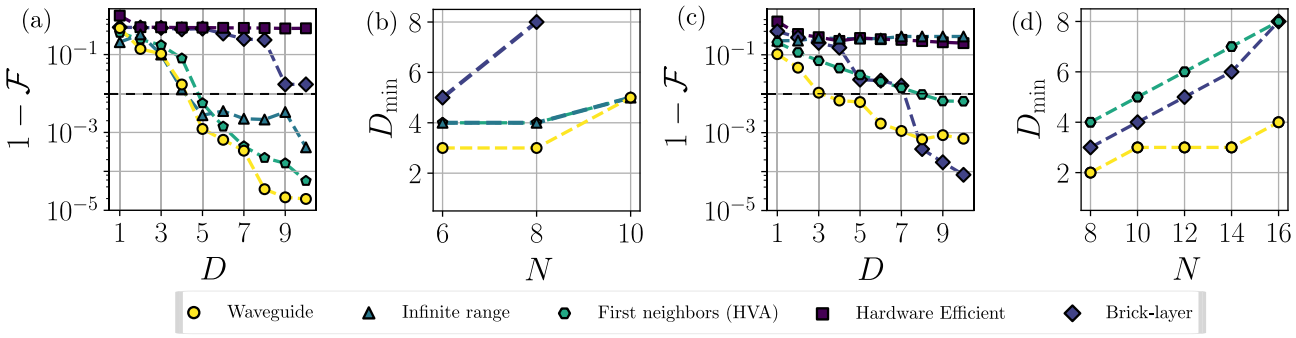

FIG. 2. (a) Infidelity $1-\mathcal{F}$ between the exact g.s. of the XXZ model and the optimized variational states obtained with different *Ansätze* (see legend below) as a function of the number of layers D for a system with $N=10$ qubits. (b) Minimum depth D required to obtain a fidelity $\mathcal{F}$ over 99% for different numbers of qubits N (note that not all the *Ansätze* reach this fidelity). (c),(d) Equivalent to (a), (b) but considering the TFIM model instead of the XXZ model. The system size in (c) is $N=16$ qubits.

concatenating single-qubit rotations along the three spatial directions, and two-qubit control-Z (CZ) as entangling gates; a brick-layer *Ansatz*, in which the entangling CZ gates are introduced sequentially and interleaved by single-qubit rotations; a first-neighbor HVA, in which the layers are given by the second-order Trotterization of the spin Hamiltonian under consideration [35]; and also against an all-to-all *Ansatz*, which is a wQED *Ansatz* in which we take $L\to\infty$. The latter allows us to discern whether a possible advantage is a consequence of the long-range character of the wQED interaction or its dynamical tunability. Additionally, its results can be of interest for cavity QED setups [84–90], where such infinite range interactions appear naturally.

We first consider the XXZ model [91],

$$H_{XXZ}=\sum_i(\sigma_x^i\sigma_x^{i+1}+\sigma_y^i\sigma_y^{i+1})-\Delta\sum_i\sigma_z^i\sigma_z^{i+1}, \quad (3)$$

at its ferromagnetic Heisenberg point $\Delta=1$. In Figs. 2(a) and 2(b) we evaluate the performance of the wQED-XX *Ansatz* of Eq. (1) (in yellow circles) against the aforementioned *Ansätze*. This wQED *Ansatz* choice is owed to the resemblance of H_{XX} and the interactions appearing in the XXZ model. To assess the *Ansätze* performance we compute the infidelity:

$$1-\mathcal{F}=1-|\langle\Psi(\boldsymbol{\Theta}_{\text{opt}})|\Psi_{\text{g.s.}}\rangle|, \quad (4)$$

with $|\Psi_{\text{g.s.}}\rangle$ the g.s. of the model, and $|\Psi(\boldsymbol{\Theta}_{\text{opt}})\rangle$ that with the lowest energy found by the VQE. In Fig. 2(a) we plot the infidelity for $N=10$ qubits as a function of the circuit depth D (i.e., the number of layers). Adding more layers typically results in better fidelities for most *Ansätze*. This is expected since deeper circuits contain more variational parameters that can help in exploring larger regions of the Hilbert space and getting closer to the g.s. [80,92]. However, we appreciate that the wQED-XX *Ansatz* performs better than the rest. To confirm this fact, we calculate the required circuit depth to obtain fidelities beyond 99% for several N's, finding that the wQED-XX *Ansatz* produces a better approximation to the g.s. with shallower circuits than the other *Ansätze* [see Fig. 2(b)]. This shallowness is advantageous because it makes the system more resilient to noise, and will require fewer measurements in the optimization loop.

This advantage is clearer when we study the transverse-field Ising model (TFIM),

$$H_{\text{TFIM}}=-\sum_i\sigma_x^i\sigma_x^{i+1}+g\sum_i\sigma_z^i, \quad (5)$$

at the critical point $g=1$. The results are shown in Figs. 2(c) and 2(d). In this case we use the wQED-I *Ansatz*, again due to the similarity between the Ising interactions appearing in H_I and those of the target problem. On top of that, it is noteworthy that here we use a global single-qubit rotation, which substantially reduces the number of parameters with respect to the other *Ansätze* [63], and simplifies the experimental implementation because one can address the emitters globally. The results of the *Ansätze* comparison are presented in Fig. 2(c). There, we fix the number of qubits at $N=16$, and show that for most *Ansätze* the infidelity decreases with the circuit depth D. Because of the particular structure of the wQED-I *Ansatz*, in this case we can benchmark the *Ansätze* for larger values of $6\le N\le 16$, for which it provides the most accurate results, especially at low circuit depths. This is confirmed in Fig. 2(d), where we plot the depth required by the *Ansätze* to achieve fidelities beyond 99%. There, the wQED-I *Ansatz* reaches the desired fidelity systematically for smaller D. It is also interesting to highlight the inferior performance of the all-to-all *Ansatz* compared with both wQED *Ansätze*. This points to the fact that it is not only the long-range character of the interaction, but also its dynamical tuning, that allows the latter to reproduce better the power-law correlations of the g.s. and thus to outperform the rest. Note that the nonmonotonic behavior of the

brick-layer *Ansatz* has been predicted before [63,80,81], and is due to the finite number of layers required ($D \sim N/2$) to establish finite correlations along the whole system [63,80,81].

Finally, we check the performance of the wQED *Ansatz* for models with long-range interactions, like the long-range transverse-field Ising model (LRTFIM):

$$H_{\mathrm{LRTFIM}} = -\sin\theta \sum_{i\neq j} \frac{1}{|i-j|^{\alpha}} \sigma_x^i \sigma_x^j + \cos\theta \sum_{i=1}^{N} \sigma_z^i. \quad (6)$$

In this case the position of the critical point depends on the power-law exponent α [93–95]: here we consider three different values $\alpha = 1/2$, 1, 3, and choose θ to be at the critical point [63] in each case. The interactions appearing in the target Hamiltonian (6) make the wQED-*I Ansatz* of Eq. (2) the natural choice for this problem. Additionally, we also compare with a modified version of the wQED-*I Ansatz* in which $W_I(T_i, L_i)$ is replaced by the product of two unitaries $\prod_{l=1}^{2} W_I(T_l, L_l)$ within each layer, and with the parameters T_l, L_l chosen in such a way that $\sum_l J_l e^{-|x_i - x_j|/L_l} \approx J_\alpha/|x_i - x_j|^{\alpha}$ approximates the power-law exponent of the target model for a given range of distances [96]. This multiexponential interaction can be realized by means of multifrequency Raman lasers, as shown in Ref. [55]. The results are summarized in Fig. 3, where Figs. 3(a)–3(c) display the infidelity as a function of the number of layers for $N = 14$ qubits and Figs. 3(d)–3(f) show the required depth to achieve a fidelity beyond 99% for different N's. The main conclusion is that, like in the previous cases, the wQED-*I Ansätze* achieves the targeted fidelities for smaller (or equal) circuit depths, even for the longer-ranged models. However, in these models the power-law wQED *Ansatz* eventually outperforms the exponential one for larger circuit depths.

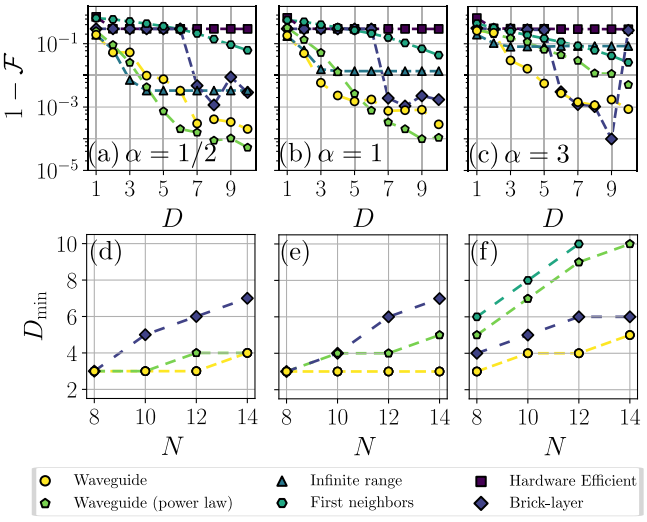

FIG. 3. (a)–(c) Infidelity $1 - \mathcal{F}$ between the exact g.s. of the LRTFIM and the optimized variational states obtained with different *Ansätze* as a function of the number of layers D for several values of the power-law exponent α. The system size is $N = 14$ qubits. (d)–(f) Minimum depth D required to obtain a fidelity $\mathcal{F}$ over 99% as a function of the number of qubits N and for different values of α.

Impact of noise.—So far we have considered an ideal noiseless situation. This is not the case of real setups where dissipation associated to the waveguide modes, disorder, and other decay channels will introduce errors. Given the variety of wQED platforms [37–54], where the most relevant errors might have a different physical origin, to study the impact of noise we use the platform-agnostic error model described in Refs. [6,63], which assumes a constant error probability $p_{1(2)}$ for each single-qubit (multiqubit) gate. We focus on the impact of noise in the VQE for the TFIM in Eq. (5) as cost function, since it is numerically easier. The results are summarized in Fig. 4, where we show the evolution of the infidelity with the number of layers for two values of $p_{1(2)}$, each pair corresponding to a different panel. Such values have been chosen in the range of gate fidelities displayed by some of the state-of-the-art NISQ devices [98,99]. We conclude that in the presence of noise the infidelity does not decrease monotonically when increasing the circuit depth. This is true for all *Ansätze*, including the wQED-*I* one. The reason behind this is that by adding more layers one introduces more variational parameters, which improves the optimization process at equal conditions, but the resulting increase in accuracy is lost at some point due to the error accumulation by the application of more gates. With this error model, the wQED-*I Ansatz* reaches the smallest infidelity. The underlying reason is a combination of its better performance at small circuit depths, and the smaller number of gates per layer with respect to the other *Ansätze*, which limits the introduction of errors. The latter will be true also for errors

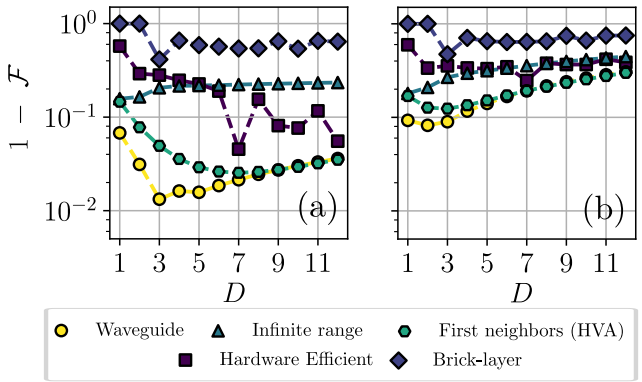

FIG. 4. (a),(b) Effects of decoherence in the infidelity $1 - \mathcal{F}$ between the exact g.s. of the TFIM and the optimized variational states obtained with different *Ansätze* as a function of the number of layers D for $N = 12$ qubits. The error probabilities for single- and two-qubit gates are, respectively, $p_1 = 10^{-5}$ and $p_2 = 5 \times 10^{-4}$ (a) and $p_1 = 10^{-4}$ and $p_2 = 5 \times 10^{-3}$ (b).

coming from imperfect gate control, which could also benefit from the smaller depth of the wQED circuits. We leave for future work the study of more refined error models devoted to each specific implementation [37–54].

Conclusions and outlook.—To summarize, we introduce a new type of VQE *Ansatz* based on the tunable-range interactions that can be engineered in wQED setups. We show that, thanks to this tunability, this *Ansatz* captures phases with long-range correlations with fewer gates and parameters than other fixed structure *Ansätze* of the literature, becoming potentially less sensitive to gate errors. While wQED is still behind in fidelities compared to variational trapped ions [12,26] or superconducting quantum simulators [6], the rapid experimental advances in the integration of emitters with photonic waveguides [37–47], microwave circuits [48–51,100], or matter waves [53,54], plus the potentialities shown in this work, place wQED simulators as promising candidates both for VQEs and also for other VQAs. For example, recent experiments in the microwave regime with up to ten qubits [51,52] have demonstrated the control of the range of the interactions and the individual atomic states, and thus have all the necessary ingredients to implement our ideas. On the other hand, quantum nanophotonic experiments [40,101,102] still need ways of reliably trapping and positioning the emitters in a scalable way. However, recent advances in optical tweezers [102] and optical guiding techniques [103] open a path to do it with atoms.

Finally, note that the idea of using the interaction range as a variational parameter can be extended to other setups where such tunable-range interactions can be engineered such as trapped ions [104–109] or multimode cavity QED setups [110]. As an outlook, we plan to extend our results to higher-dimensional models [111], where such tunable exponential [56,112] and power-law interactions can also be obtained [113–117], models with high-dimensional spins [85,118,119], as well as to design adaptative *Ansätze* [120–125] based on wQED interactions, which is another active area of research within variational quantum computing.

The authors acknowledge support from the Proyecto Sinérgico CAM 2020 Y2020/TCS-6545 (NanoQuCo-CM), from the CSIC Research Platform on Quantum Technologies PTI-001, and from Spanish Projects No. PID2021-127968NB-I00 and No. TED2021-130552B-C22 (funded by MCIN/AEI/10.13039/501100011033/FEDER, EU and MCIN/AEI/10.13039/501100011033, respectively). The authors also acknowledge Centro de Supercomputación de Galicia (CESGA) who provided access to the supercomputer FinisTerrae for performing numerical simulations. A. M. H. acknowledges support from Fundación General CSIC's ComFuturo programme which has received funding from the European Union's Horizon 2020 research and innovation programme under the Marie Skłodowska-Curie Grant Agreement No. 101034263. A. G.-T. also acknowledges support from a 2022 Leonardo Grant for Researchers and Cultural Creators, BBVA Foundation, and thanks X. Zhang for insightful discussions on the physical implementation of the ideas and for a critical reading of the manuscript.

*a.gonzalez.tudela@csic.es

[1] M. Cerezo, A. Arrasmith, R. Babbush, S. C. Benjamin, S. Endo, K. Fujii, J. R. McClean, K. Mitarai, X. Yuan, L. Cincio, and P. J. Coles, Nat. Phys. Rev. **3**, 625 (2021).
[2] K. Bharti, A. Cervera-Lierta, T. H. Kyaw, T. Haug, S. Alperin-Lea, A. Anand, M. Degroote, H. Heimonen, J. S. Kottmann, T. Menke, W. K. Mok, S. Sim, L. C. Kwek, and A. Aspuru-Guzik, Rev. Mod. Phys. **94**, 015004 (2022).
[3] J. Preskill, Quantum **2**, 79 (2018).
[4] J. Tilly, H. Chen, S. Cao, D. Picozzi, K. Setia, Y. Li, E. Grant, L. Wossnig, I. Rungger, G. H. Booth, and J. Tennyson, Phys. Rep. **986**, 1 (2022).
[5] A. Peruzzo, J. McClean, P. Shadbolt, M.-H. Yung, X.-Q. Zhou, P. J. Love, A. Aspuru-Guzik, and J. L. O'brien, Nat. Commun. **5**, 4213 (2014).
[6] A. Kandala, A. Mezzacapo, K. Temme, M. Takita, M. Brink, J. M. Chow, and J. M. Gambetta, Nature (London) **549**, 242 (2017).
[7] G. A. Quantum, Science **369**, 1084 (2020).
[8] J. Lee, W. J. Huggins, M. Head-Gordon, and K. B. Whaley, J. Chem. Theory Comput. **15**, 311 (2019).
[9] Y. Matsuzawa and Y. Kurashige, J. Chem. Theory Comput. **16**, 944 (2020).
[10] I. D. Kivlichan, N. Wiebe, R. Babbush, and A. Aspuru-Guzik, J. Phys. A **50**, 305301 (2017).
[11] K. Setia, S. Bravyi, A. Mezzacapo, and J. D. Whitfield, Phys. Rev. Res. **1**, 033033 (2019).
[12] C. Kokail, C. Maier, R. van Bijnen, T. Brydges, M. K. Joshi, P. Jurcevic, C. A. Muschik, P. Silvi, R. Blatt, C. F. Roos, and P. Zoller, Nature (London) **569**, 355 (2019).
[13] A. Yamamoto, Phys. Rev. D **104**, 014506 (2021).
[14] R. Irmejs, M. C. Banuls, and J. I. Cirac, arXiv:2206.08909.
[15] D. Paulson, L. Dellantonio, J. F. Haase, A. Celi, A. Kan, A. Jena, C. Kokail, R. van Bijnen, K. Jansen, P. Zoller, and C. A. Muschik, PRX Quantum **2**, 030334 (2021).
[16] A. N. Ciavarella and I. A. Chernyshev, Phys. Rev. D **105**, 074504 (2022).
[17] E. Farhi, J. Goldstone, and S. Gutmann, arXiv:1411.4028.
[18] C. Y.-Y. Lin and Y. Zhu, arXiv:1601.01744.
[19] N. Moll, P. Barkoutsos, L. S. Bishop, J. M. Chow, A. Cross, D. J. Egger, S. Filipp, A. Fuhrer, J. M. Gambetta, M. Ganzhorn, A. Kandala, A. Mezzacapo, P. Müller, W. Riess, G. Salis, J. Smolin, I. Tavernelli, and K. Temme, Quantum Sci. Technol. **3**, 030503 (2018).
[20] B. X. Wang and C. Y. Zhao, Phys. Rev. A **98**, 023808 (2018).
[21] N. Lacroix, C. Hellings, C. K. Andersen, A. Di Paolo, A. Remm, S. Lazar, S. Krinner, G. J. Norris, M. Gabureac,

J. Heinsoo, A. Blais, C. Eichler, and A. Wallraff, PRX Quantum **1**, 020304 (2020).
[22] M. P. Harrigan *et al.*, Nat. Phys. **17**, 332 (2021).
[23] V. Havlíček, A. D. Córcoles, K. Temme, A. W. Harrow, A. Kandala, J. M. Chow, and J. M. Gambetta, Nature (London) **567**, 209 (2019).
[24] S. Johri, S. Debnath, A. Mocherla, A. Singk, A. Prakash, J. Kim, and I. Kerenidis, npj Quantum Inf. **7**, 122 (2021).
[25] B. Koczor, S. Endo, T. Jones, Y. Matsuzaki, and S. C. Benjamin, New J. Phys. **22**, 083038 (2020).
[26] R. Kaubruegger, D. V. Vasilyev, M. Schulte, K. Hammerer, and P. Zoller, Phys. Rev. X **11**, 041045 (2021).
[27] Z. Ma, P. Gokhale, T. X. Zheng, S. Zhou, X. Yu, L. Jiang, P. Maurer, and F. T. Chong, in *2021 IEEE International Conference on Quantum Computing and Engineering (QCE), Broomfield, CO, USA* (2021), pp. 419–430.
[28] J. L. Beckey, M. Cerezo, A. Sone, and P. J. Coles, Phys. Rev. Res. **4**, 013083 (2022).
[29] J. R. McClean, S. Boixo, V. N. Smelyanskiy, R. Babbush, and H. Neven, Nat. Commun. **9**, 4812 (2018).
[30] Z. Holmes, K. Sharma, M. Cerezo, and P. J. Coles, Phys. Rev. X Quantum **3**, 010313 (2022).
[31] D. Wecker, M. B. Hastings, and M. Troyer, Phys. Rev. A **92**, 042303 (2015).
[32] J. M. Reiner, F. Wilhelm-Mauch, G. Schön, and M. Marthaler, Quantum Sci. Technol. **4**, 035005 (2019).
[33] G. Verdon, M. Broughton, J. R. McClean, K. J. Sung, R. Babbush, Z. Jiang, H. Neven, and M. Mohseni, arXiv:1907.05415.
[34] A. A. Mele, G. B. Mbeng, G. E. Santoro, M. Collura, and P. Torta, Phys. Rev. A **106**, 060401 (2021).
[35] R. Wiersema, C. Zhou, Y. de Sereville, J. F. Carrasquilla, Y. B. Kim, and H. Yuen, PRX Quantum **1**, 020319 (2020).
[36] G. Pagano, A. Bapat, P. Becker, K. S. Collins, A. De, P. W. Hess, H. B. Kaplan, A. Kyprianidis, W. L. Tan, C. Baldwin, L. T. Brady, A. Deshpande, F. Liu, S. Jordan, A. V. Gorshkov, and C. Monroe, Proc. Natl. Acad. Sci. U.S.A. **117**, 25396 (2020).
[37] A. Goban, C.-L. Hung, S.-P. Yu, J. D. Hood, J. A. Muniz, J. H. Lee, M. J. Martin, A. C. McClung, K. S. Choi, D. E. Chang, O. Painter, and H. J. Kimblemblrm, Nat. Commun. **5**, 3808 (2014).
[38] A. Goban, C.-L. Hung, J. D. Hood, S.-P. Yu, J. A. Muniz, O. Painter, and H. J. Kimble, Phys. Rev. Lett. **115**, 063601 (2015).
[39] J. D. Hood, A. Goban, A. Asenjo-Garcia, M. Lu, S.-P. Yu, D. E. Chang, and H. J. Kimble, Proc. Natl. Acad. Sci. U.S.A. **113**, 10507 (2016).
[40] P. Samutpraphoot, T. Dordevic, P. L. Ocola, H. Bernien, C. Senko, V. Vuletić, and M. D. Lukin, Phys. Rev. Lett. **124**, 063602 (2020).
[41] A. Laucht, S. Pütz, T. Günthner, N. Hauke, R. Saive, S. Frédérick, M. Bichler, M.-C. Amann, A. W. Holleitner, M. Kaniber, and J. J. Finley, Phys. Rev. X **2**, 011014 (2012).
[42] R. E. Evans, M. K. Bhaskar, D. D. Sukachev, C. T. Nguyen, A. Sipahigil, M. J. Burek, B. Machielse, G. H. Zhang, A. S. Zibrov, E. Bielejec *et al.*, Science **362**, 662 (2018).
[43] M. H. Appel, A. Tiranov, A. Javadi, M. C. Löbl, Y. Wang, S. Scholz, A. D. Wieck, A. Ludwig, R. J. Warburton, and P. Lodahl, Phys. Rev. Lett. **126**, 013602 (2021).
[44] A. Tiranov, V. Angelopoulou, C. J. van Diepen, B. Schrinski, O. A. D. Sandberg, Y. Wang, L. Midolo, S. Scholz, A. D. Wieck, A. Ludwig, A. S. Sørensen, and P. Lodahl, Science **379**, 389 (2023).
[45] B. Machielse, S. Bogdanovic, S. Meesala, S. Gauthier, M. J. Burek, G. Joe, M. Chalupnik, Y. I. Sohn, J. Holzgrafe, R. E. Evans, C. Chia, H. Atikian, M. K. Bhaskar, D. D. Sukachev, L. Shao, S. Maity, M. D. Lukin, and M. Lončar, Phys. Rev. X **9**, 031022 (2019).
[46] A. E. Rugar, C. Dory, S. Aghaeimeibodi, H. Lu, S. Sun, S. D. Mishra, Z. X. Shen, N. A. Melosh, and J. Vučković, ACS Photonics **7**, 2356 (2020).
[47] A. E. Rugar, S. Aghaeimeibodi, D. Riedel, C. Dory, H. Lu, P. J. McQuade, Z. X. Shen, N. A. Melosh, and J. Vučković, Phys. Rev. X **11**, 031021 (2021).
[48] Y. Liu and A. A. Houck, Nat. Phys. **13**, 48 (2017).
[49] M. Mirhosseini, E. Kim, V. S. Ferreira, M. Kalaee, A. Sipahigil, A. J. Keller, and O. Painter, Nat. Commun. **9**, 3706 (2018).
[50] N. M. Sundaresan, R. Lundgren, G. Zhu, A. V. Gorshkov, and A. A. Houck, Phys. Rev. X **9**, 011021 (2019).
[51] M. Scigliuzzo, G. Calajò, F. Ciccarello, D. Perez Lozano, A. Bengtsson, P. Scarlino, A. Wallraff, D. Chang, P. Delsing, and S. Gasparinetti, Phys. Rev. X **12**, 031036 (2022).
[52] X. Zhang, E. Kim, D. K. Mark, S. Choi, and O. Painter, Science **379**, 278 (2023).
[53] L. Krinner, M. Stewart, A. Pazmino, J. Kwon, and D. Schneble, Nature (London) **559**, 589 (2018).
[54] J. Kwon, Y. Kim, A. Lanuza, and D. Schneble, Nat. Phys. **18**, 657 (2022).
[55] J. S. Douglas, H. Habibian, C.-L. Hung, A. V. Gorshkov, H. J. Kimble, and D. E. Chang, Nat. Photonics **9**, 326 (2015).
[56] A. González-Tudela, C.-L. Hung, D. Chang, J. Cirac, and H. Kimble, Nat. Photonics **9**, 320 (2015).
[57] C.-L. Hung, A. González-Tudela, J. Ignacio Cirac, and H. Kimble, Proc. Natl. Acad. Sci. U.S.A. **113** (2016).
[58] J. D. Joannopoulos, S. G. Johnson, J. N. Winn, and R. D. Meade, *Photonic Crystals: Molding the Flow of Light* (Princeton University Press, Princeton, 2011).
[59] D. E. Chang, J. S. Douglas, A. González-Tudela, C.-L. Hung, and H. J. Kimble, Rev. Mod. Phys. **90**, 031002 (2018).
[60] V. P. Bykov, Sov. J. Quantum Electron. **4**, 861 (1975).
[61] S. John and J. Wang, Phys. Rev. Lett. **64**, 2418 (1990).
[62] G. Kurizki, Phys. Rev. A **42**, 2915 (1990).
[63] See Supplemental Material at http://link.aps.org/supplemental/10.1103/PhysRevLett.131.073602 for more details on (i) waveguide-mediated interactions, (ii) the *Ansätze* and optimization algorithms that we use in the main text, and (iii) the error modeling, which also includes Refs. [64–79].
[64] B. Peropadre, D. Zueco, F. Wulschner, F. Deppe, A. Marx, R. Gross, and J. J. García-Ripoll, Phys. Rev. B **87**, 134504 (2013).

[65] Y. Chen *et al.*, Phys. Rev. Lett. **113**, 220502 (2014).
[66] P. Roushan *et al.*, Nat. Phys. **13**, 146 (2017).
[67] I. de Vega, D. Porras, and J. Ignacio Cirac, Phys. Rev. Lett. **101**, 260404 (2008).
[68] C. Navarrete-Benlloch, I. de Vega, D. Porras, and J. I. Cirac, New J. Phys. **13**, 023024 (2011).
[69] S. Sim, P. D. Johnson, A. Aspuru-Guzik, S. Sim, P. D. Johnson, and A. Aspuru-Guzik, Adv. Quantum Technol. **2**, 1900070 (2019).
[70] K. Nakaji and N. Yamamoto, Quantum **5**, 434 (2021).
[71] G. Mussardo, *Statistical Field Theory: An Introduction to Exactly Solved Models in Statistical Physics* (Oxford University Press, New York, 2020).
[72] T. Koffel, M. Lewenstein, and L. Tagliacozzo, Phys. Rev. Lett. **109**, 267203 (2012).
[73] J. Haferkamp, P. Faist, N. B. Kothakonda, J. Eisert, and N. Yunger Halpern, Nat. Phys. **18**, 528 (2022).
[74] S. Bravyi, M. B. Hastings, and F. Verstraete, Phys. Rev. Lett. **97**, 050401 (2006).
[75] V. Bergholm *et al.*, arXiv:1811.04968.
[76] A. Paszke *et al.*, arXiv:1912.01703.
[77] D. P. Kingma and J. L. Ba, in *Adam: A Method for Stochastic Optimization (Conference Paper at the 3rd International Conference for Learning Representations, San Diego, 2015)*, arXiv:1412.6980.
[78] S. Barison, F. Vicentini, I. Cirac, and G. Carleo, Phys. Rev. Res. **4**, 043161 (2022).
[79] Y. Wang, M. J. Gullans, X. Na, and A. V. Gorshkov, Phys. Rev. Res. **4**, 023014 (2022).
[80] C. Bravo-Prieto, J. Lumbreras-Zarapico, L. Tagliacozzo, and J. I. Latorre, Quantum **4**, 272 (2020).
[81] B. Jobst, A. Smith, and F. Pollmann, Phys. Rev. Res. **4**, 033118 (2022).
[82] S. Roca-Jerat, T. Sancho-Lorente, J. Román-Roche, and D. Zueco, arXiv:2301.04671.
[83] A. Garcia-Saez and J. I. Latorre, arXiv:1806.02287.
[84] H. Ritsch, P. Domokos, F. Brennecke, and T. Esslinger, Rev. Mod. Phys. **85**, 553 (2013).
[85] E. J. Davis, G. Bentsen, L. Homeier, T. Li, and M. H. Schleier-Smith, Phys. Rev. Lett. **122**, 010405 (2019).
[86] A. Periwal, E. S. Cooper, P. Kunkel, J. F. Wienand, E. J. Davis, and M. Schleier-Smith, Nature (London) **600**, 630 (2021).
[87] Z. Li, B. Braverman, S. Colombo, C. Shu, A. Kawasaki, A. F. Adiyatullin, E. Pedrozo-Peñafiel, E. Mendez, and V. Vuletić, PRX Quantum **3**, 020308 (2022).
[88] J. Ramette, J. Sinclair, Z. Vendeiro, A. Rudelis, M. Cetina, and V. Vuletić, PRX Quantum **3**, 010344 (2022).
[89] G. P. Greve, C. Luo, B. Wu, and J. K. Thompson, Nature (London) **610**, 472 (2022).
[90] O. Hosten, N. J. Engelsen, R. Krishnakumar, and M. A. Kasevich, Nature (London) **529**, 505 (2016).
[91] A. Langari, Phys. Rev. B **58**, 14467 (1998).
[92] M. Larocca, N. Ju, D. García-Martín, P. J. Coles, and M. Cerezo, Nat. Comput. Sci. **3**, 542 (2023).
[93] D. Ruelle, Commun. Math. Phys. **9**, 267 (1968).
[94] F. J. Dyson, Commun. Math. Phys. **12**, 91 (1969).
[95] A. Dutta and J. K. Bhattacharjee, Phys. Rev. B **64**, 184106 (2001).
[96] These parameters can always by found by fitting the power law with exponentials [97].
[97] B. Pirvu, V. Murg, J. I. Cirac, and F. Verstraete, New J. Phys. **12**, 025012 (2010).
[98] S. A. Moses *et al.*, arXiv:2305.03828.
[99] Y. Kim *et al.*, Nature (London) **618**, 500 (2023).
[100] H. Zhang, J. Li, H. Jiang, N. Li, J. Wang, J. Xu, C. Zhu, and Y. Yang, Phys. Rev. A **105**, 053703 (2022).
[101] A. Tiranov, V. Angelopoulou, C. J. van Diepen, B. Schrinski, O. A. Dall'Alba Sandberg, Y. Wang, L. Midolo, S. Scholz, A. D. Wieck, A. Ludwig, A. S. Sørensen, and P. Lodahl, Science **379**, 389 (2023).
[102] T. Dordevic, P. Samutpraphoot, P. L. Ocola, H. Bernien, B. Grinkemeyer, I. Dimitrova, V. Vuletić, and M. D. Lukin, Science **373**, 1511 (2021).
[103] X. Zhou, H. Tamura, T.-H. Chang, and C.-L. Hung, Phys. Rev. Lett. **130**, 103601 (2023).
[104] D. Porras and J. I. Cirac, Phys. Rev. Lett. **92**, 207901 (2004).
[105] P. Nevado and D. Porras, Phys. Rev. A **93**, 013625 (2016).
[106] P. Richerme, Z.-X. Gong, A. Lee, C. Senko, J. Smith, M. Foss-Feig, S. Michalakis, A. V. Gorshkov, and C. Monroe, Nature (London) **511**, 198 (2014).
[107] P. Jurcevic, B. P. Lanyon, P. Hauke, C. Hempel, P. Zoller, R. Blatt, and C. F. Roos, Nature (London) **511**, 202 (2014).
[108] M. K. Joshi, A. Elben, B. Vermersch, T. Brydges, C. Maier, P. Zoller, R. Blatt, and C. F. Roos, Phys. Rev. Lett. **124**, 240505 (2020).
[109] C. Monroe, W. C. Campbell, L. M. Duan, Z. X. Gong, A. V. Gorshkov, P. W. Hess, R. Islam, K. Kim, N. M. Linke, G. Pagano, P. Richerme, C. Senko, and N. Y. Yao, Rev. Mod. Phys. **93**, 025001 (2021).
[110] V. D. Vaidya, Y. Guo, R. M. Kroeze, K. E. Ballantine, A. J. Kollár, J. Keeling, and B. L. Lev, Phys. Rev. X **8**, 011002 (2018).
[111] T. Armon, S. Ashkenazi, G. García-Moreno, A. González-Tudela, and E. Zohar, Phys. Rev. Lett. **127**, 250501 (2021).
[112] A. González-Tudela and F. Galve, ACS Photonics **6**, 221 (2018).
[113] J. Perczel and M. D. Lukin, Phys. Rev. A **101**, 033822 (2020).
[114] A. González-Tudela and J. I. Cirac, Phys. Rev. A **97**, 043831 (2018).
[115] J. Redondo-Yuste, M. Blanco De Paz, P. A. Huidobro, and A. González-Tudela, New J. Phys. **23**, 103018 (2021).
[116] I. n. García-Elcano, A. González-Tudela, and J. Bravo-Abad, Phys. Rev. Lett. **125**, 163602 (2020).
[117] E. P. Navarro-Barón, H. Vinck-Posada, and A. González-Tudela, ACS Photonics **8**, 3209 (2021).
[118] A. P. Orioli, J. K. Thompson, and A. M. Rey, Phys. Rev. X **12**, 011054 (2022).
[119] C. Tabares, E. Zohar, and A. González-Tudela, Phys. Rev. A **106**, 033705 (2022).
[120] L. Zhu, H. L. Tang, G. S. Barron, F. A. Calderon-Vargas, N. J. Mayhall, E. Barnes, and S. E. Economou, Phys. Rev. Res. **4**, 033029 (2022).
[121] H. R. Grimsley, S. E. Economou, E. Barnes, and N. J. Mayhall, Nat. Commun. **10**, 3007 (2019).

[122] Y. X. Yao, N. Gomes, F. Zhang, C. Z. Wang, K. M. Ho, T. Iadecola, and P. P. Orth, PRX Quantum **2**, 030307 (2021).
[123] X. H. H. Zhang and H. U. Baranger, Phys. Rev. A **103**, 033711 (2021).
[124] D. Claudino, J. Wright, A. J. McCaskey, and T. S. Humble, Front. Chem. **8**, 1152 (2020).
[125] H. L. Tang, V. O. Shkolnikov, G. S. Barron, H. R. Grimsley, N. J. Mayhall, E. Barnes, and S. E. Economou, PRX Quantum **2**, 020310 (2021).